United Journal of Nanotechnology and Pharmaceutics

The Comparison and Evaluation of Thermal Behavior, Pore Morphology, Permeability Properties, and Tensile Behavior Effects on Melt Stretching Calcium Carbonate/ Talc- Polypropylene-Based Microporous Membranes

K. Habibi[1]*, Pilar Castejón[1], A.B. Martínez[1], D. Arencón osuna[1]*

[1]Centre Català del Plàstic. Universitat Politècnica de Catalunya. C/Colom 114, E-08222 Terrassa, Spain.

Author Biography

Dr. Kian Habibi

Dr. Kian Habibi has a Ph.D. in Petroleum Engineering and he is an independent researcher, consultant, and Society of Petroleum Engineers volunteer for Ambassador lecturer, and a member of SPE's young professionals. He is also a member of the editorial board of Petroleum Engineering Science and Journal. He is a member of the American Membrane Association for more than 4 years. Dr. Kian Habibi has published five books, and he has published articles in several prominent journals, he presented some of his works as papers at various national and international conferences as well. He also has ten years of experience working for the oil and gas industry.

*Corresponding Aurthor: Dr. Kian Habibi
Centre Català del Plàstic. Universitat Politècnica de Catalunya. C/ Colom 114, E-08222 Terrassa, Spain.

Article Information
Article Type: Review Article
Article Received: 06-18-2021
Article Accepted: 06-25-2020
Article Published: 06-28-2021
Vol:1, Issue:1

OPEN ACCESS

Keywords:
Microporous Membranes; Calcium Carbonate Morphology; Talc Size; MEAUS Process; Amorphous Tie Chains; Elastic Modulus

Abstract

Micro-sized calcium carbonate and several commercial grades of talc were selected to develop polypropylene-based microporous membranes through the MEAUS process (melt extrusion – annealing – uniaxial strain). Different filler percentages were added to polypropylene (1, 5, 10 wt. % calcium carbonate/talc). To analyze the effect of the calcium carbonate/talc, and content of the obtained membranes, parameters such as draw ratio during extrusion, annealing temperature, strain rate, and strain extension were kept constant. Talc membranes showed that the small particle size and high aspect ratio tend to provide membranes with fine pore distribution, high porous area, and high Gurley permeability values, and calcium carbonate membranes demonstrated that the stress applied involved a pre-orientation of the amorphous tie chains before crystal chain unfolding, which can be related to the first yield point. A logical pattern of increasing elastic modulus as filler content does is found in calcium carbonate compounds.

Introduction

Membranes are increasingly employed for separation processes in many areas such as chemical technology, and they are used in a broad range of applications. The most important property of membranes is their ability to control the rate of permeation of different species the key property that is exploited is the ability of a membrane to control the permeation rate of a chemical species through the membrane.

Separation of well stream gas from free liquids is the first and most critical stage of field-processing operations is another application of membranes. The composition of the fluid mixture and pressure determine what type and size of the separator are required [1, 2]

Polymeric membranes are made through various techniques such as phase separation, track etching, leaching, thermal precipitation, and stretching. In phase inversion, the polymeric raw material is mixed with a solvent as well as a no solvent and during phase separation, a first phase rich in polymer forms the matrix and the second phase poor in polymer creates the pores. In track etching, the polymeric film is irradiated to create tracks followed by acid etching. The leaching technique is based on extrusion of the polymeric row material added with the solid particles followed by the extrusion of the solid, leading to pores formation. In thermal precipitation cooling of a mixture of a polymer with a solvent is applied to enable phase separation followed by extrusion of the solvent. The stretching technique is based on the stretching of a polymer film containing a dispersed phase whereupon stretching pores are created due to stress concentration at the interface of these sites, or stretching specific crystalline morphology [1-5]. Phase separation is the most employed technology to produce polymeric membranes. Nevertheless, environmental concerns have to be taken into account, such as solvent contamination and costly solvent recovery is two drawbacks for solution casting, although some improvements have been made in the recent decade.

In the present work, we have employed a technology based on polymer stretching, called MEAUS (melt extrusion – annealing – uniaxial

Citetion: Kian Habibi. / United Journal of Nanotechnology and Pharmaceutics 1(2021): 1-11

strain). This procedure applies to semi-crystalline polymers, based on (1) the stretching of a thin film with a row nucleated lamellar structure (2) annealing of the film to thicken the lamellae, and (3) stretching of the film at a low temperature to create voids and then stretching at high temperature to enlarge the pores. In the MEAUS process, the extrusion and production of the precursor films is a delicate process since the samples should be produced under a high draw ratio and cooling rates. Obtaining a very uniform film is a major concern since any non-uniformity and thickness variations cause irregularities in the stress distribution. This method is relatively less expensive and there is no solvent contamination. Some drawbacks of the technology and industrial market of these products are the difficulty to have a homogenous distribution of the pore morphology created, and the narrow range of polymers that can create the initial row-lamellar structure, being the most employed in the industry polypropylene.

The research group of Ajji [6], Caihong [7] are the ones performed among several works in the literature by focused mainly on the use of neat polyolefins. However, only a few works dealing with the filled polyolefin. Nakamura and Nago [8, 9], created the pores through debonding of calcium carbonate from the polymeric matrix and also evaluated the dependence of properties of the microporous polypropylene sheets on stretching degree. Saffar *et al* [10], developed polypropylene microporous hydrophilic membranes, and also changes in the crystalline structure and membrane performance were investigated in detail to optimize annealing and stretching conditions. The use of mineral fillers can provide an increase in rigidness to the membrane, an enhancement of the hydrophilic surface characteristic, and also can affect the final porous morphology of the membranes, as most of the fillers have some nucleate ability in the crystallization processes of polyolefins [8-12].

The largest application, currently under development, is the production of CO_2 from flue gases from gas-fired cogeneration plants and re-use in greenhouses. Captured CO_2 utilized for EOR (Enhanced oil recovery) at mature oil fields in the Gulf Coast region. This CO_2 capture plant consists of pre-treatment, CO_2 absorption, and regeneration, CO_2 compression with dehydration, and a utility system.

Membrane gas absorption based on the novel absorption liquids and porous polyolefin membranes is an efficient technique for the removal of sulfur dioxide from various burning flare gases. A feasibility implement has demonstrated that sulfur dioxide can be captured economically from flue gas on a large scale.

Caihong *et al* [13], used magnesium sulfate whiskers as a filler and indicated that with increasing $MgSO_4$ whiskers content the porosity of the stretched microporous membranes decreased, whereas the Gurley value showed an increase in values, they also showed that the introduction of $MgSO_4$ up to 10 wt. % did not induce pronounced changes in the pore structure and air permeability properties of the stretched microporous membranes.

Cai *et al* [14], showed that the introduction of silicon dioxide into polypropylene microporous membrane leads to the improvement of the mean pore diameter of the stretched microporous membrane, also they showed that the crystalline orientation degree of precursor film was decreased by adding dioxide into polypropylene, and the Gurley value (characterizing the air permeability) decreased.

Talc, along with calcium carbonate, is one of the most employed fillers in the plastic industry, so it offers an interesting alternative in the development of membranes used in the oil separator industry. Talc has a well-known nucleating activity on the crystallization of polypropylene [15, 16] and hydrophilicity.

Talc, $Mg_3Si_4O_{10}(OH)_2$ is a trioctahedral phyllosilicate, macroscopically hydrophobic as it floats naturally with no layer charge [17,18]. However, upon outgassing, Controlled rate thermal analysis measurements coupled with mass spectrometric analyses show that different surface species (water, nitrogen, carbon dioxide, and organic molecules) are released from the talc surface [17]. The specific interactions suppress by fluorine atoms as substitution of a hydroxyl group which this assignment confirmed by the adsorption of water and nitrogen on synthetic fluorinated talc.

In this paper, the key point of this work is the combination of an advanced modification of the extrusion process (rapid air cooling) of the extruded exit along with the addition of calcium carbonate and talc as mineral fillers. Micro-sized calcium carbonate and several grades of talc are added at a different concentration to polypropylene, to analyze the crystalline orientation, membrane morphology, thermal behavior, membrane permeability, and mechanical properties of the precursor films, and evaluation of the influence of the cold and hot strain stages of MEAUS process on the permeability and mechanical properties of the membranes.

2. Materials

A commercial extrusion grade with tradename PP020 kindly supplied by Repsol S.A. has been selected with the melt flow rate (230 °C, 2.16 kg) was 1.0 $dg{\cdot}min^{-1}$, Average number and mass molecular weights were Mn =119 $kg{\cdot}mol^{-1}$ and MW = 659 $kg{\cdot}mol^{-1}$ respectively, showing a monomodal mass molecular weight distribution. As filler micro-sized (4µm average size) ultrafine surface-treated precipitated calcium carbonate (Reverté Calcium Carbonates) and five different commercial talc grades differing in particle size were added, morphology and specific surface area were kindly supplied by Imerys Talc. Micrographs accounting for calcium carbonate and talc morphology are depicted in Figure 1.

3. Experimental procedure

3.1 Film extrusion and precursor preparation

Polypropylene/calcium carbonate films (1, 5, 10 wt. % calcium carbonate) which are called C1, C5 and C10 and polypropylene/talc films (1, 5, 10 wt.% talc) were prepared by melt mixing using co-rotating twin-screw extruder (length/diameter = 36, diameter = 25 mm) (Figure 2), At the end of the extruder, a rectangular cross-section die was adapted, with nominal dimensions 122 mm x 1.9 mm. A system of two air knives was mounted close to the die to provide air to the film surface right at the exit of the die and get a fast cooling. After the air knife, a three-calander system pulled the cooled film, providing a nominal draw ratio of 70. The nominal thickness of the films ranged between 25-35 µm.

Figure 1: Morphological differences of the employed commercial grades of calcium carbonate and talc. Magnification ×1,000, 10 μm

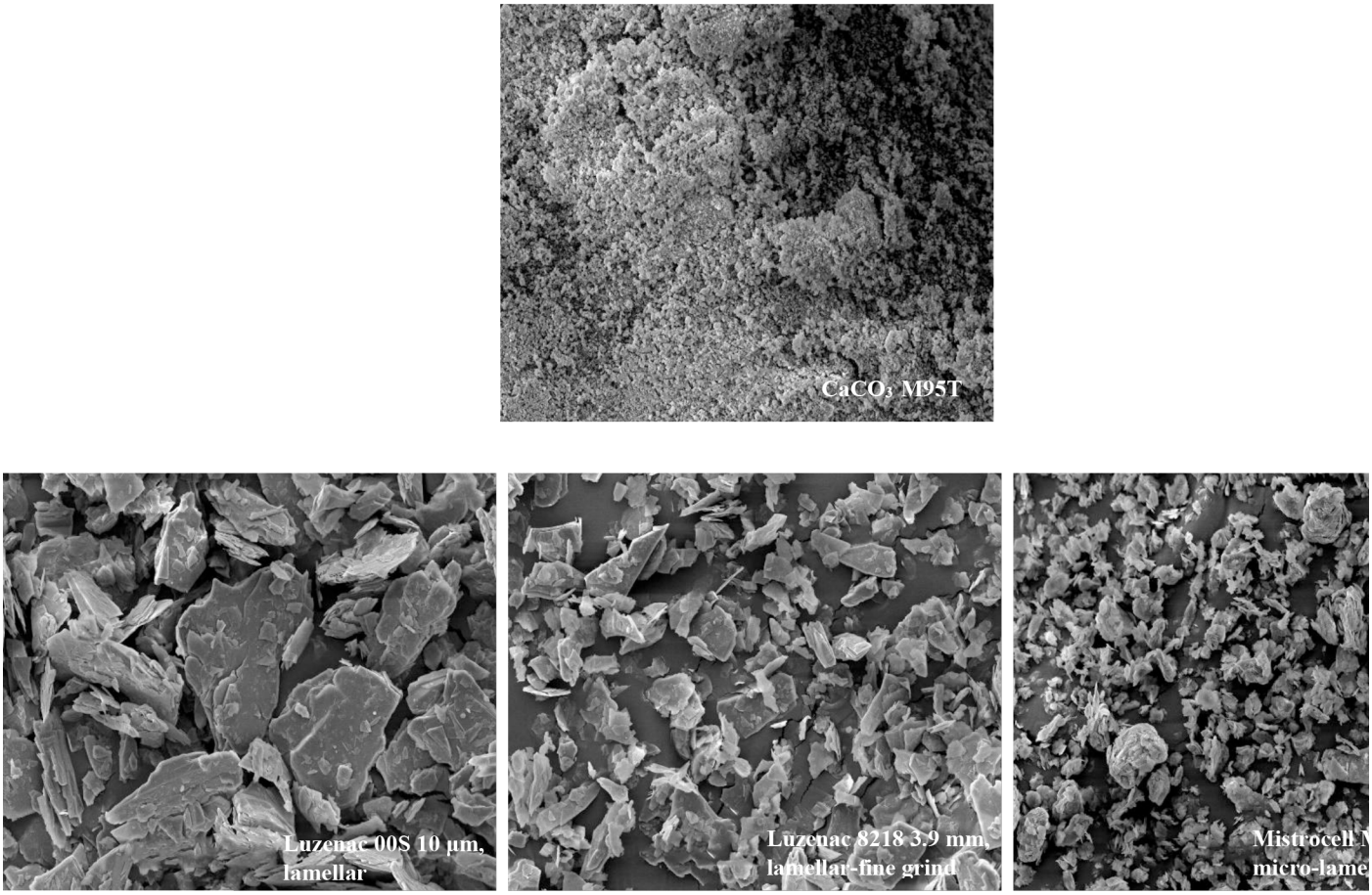

Figure 2: Summary outline of the precursor film manufacturing process

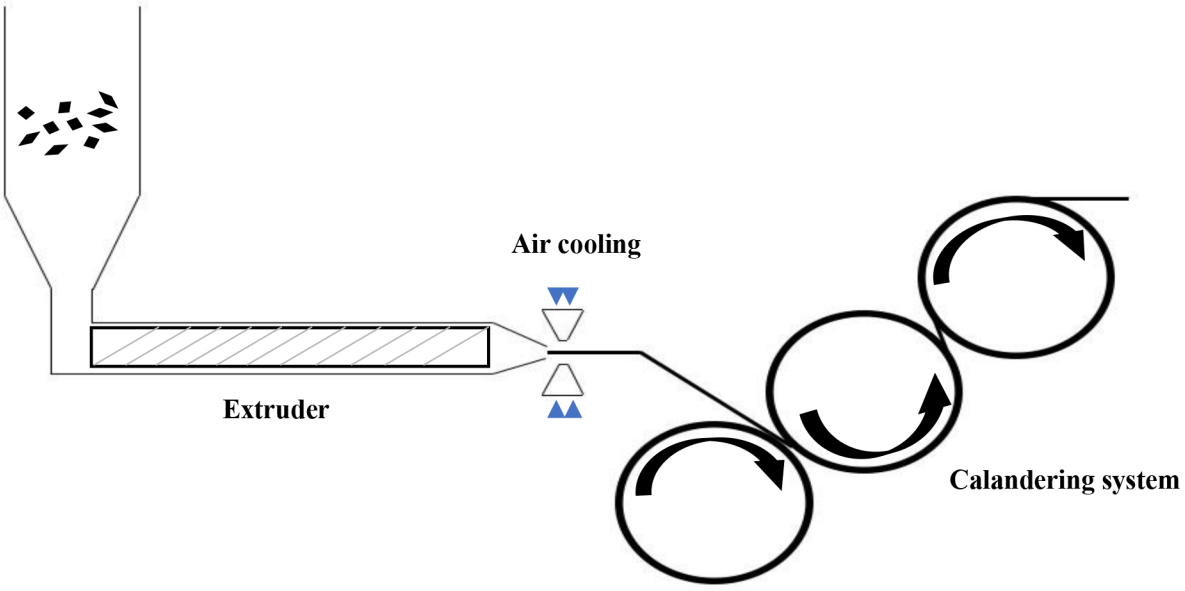

All the extruded films were annealed at three different temperatures 90, 115, 140 ºC for 15 minutes in an oven. The uniaxial strain on these rectangular samples was performed in a universal testing machine Galdabini Sun 2500, dotted with a load cell of 1 kN and a climatic chamber.

3.2 Polarized Fourier Transform Infrared spectroscopy

Infrared spectra were obtained using a spectrophotometer FT-IR Perkin Elmer Spectrum 1000 (resolution 1 cm^{-1}), equipped with a light polarizer. On the other hand, the absorbance determined with polarized light at 0º is parallel (A||) to the extrusion flow of the precursor film. On the other hand, the absorbance determined with polarized light at 90º is perpendicular (A□) to the extrusion flow. With these values, the dichroic relationship (D) could be obtained [19]:

$$D = \frac{A_{\parallel}}{A_{\perp}} \quad \text{Eq 1}$$

For polypropylene, the crystalline phase orientation (F_c) is obtained from the values of absorbance of the band at 998 cm^{-1} [6, 20], measured at 0° and 90°, from Herman expression [20].

$$F = \frac{D-1}{D+2} \quad \text{Eq 2}$$

The average orientation function (F_{av}) was obtained from Herman expression, from the absorbance signal at 972 cm^{-1} [19]. The orientation of the amorphous phase (F_{am}) can then be calculated according to:

$$F_{av} = X_m F_c + (1 - X_m)F_{am} \quad \text{Eq 3}$$

Where X_c is the degree of the crystallinity that was obtained through differential scanning calorimetry.

3.3 Thermal analysis

DSC was employed for several aims. Firstly, to determine the nucleating activity of calcium carbonate and talc on polypropylene. Secondly, to analyze the evolution of the melting peak of membranes, to get information about the structural changes in the different stages of MEAUS processing. A TA DSC Q 1000 equipment was employed. The sample weight was approximately 5 - 7 mg. A heating cycle from 30 to 200°C at 20°C/min was performed on the membranes. For comparison purposes, pellets of the different compounds were kept for 3 min at 200°C, cooled to 30°C at 20°C/min and finally heated from 30 to 200°C at 20°C/min. The alleged crystallinity results were obtained using the heat of fusion of 207.1 J/g for theoretically fully crystalline polypropylene [21].

3.4 Morphology

Scanning electron microscopy was employed (JEOL JSM-5610) for the analysis of the precursor pore structure. The precursors were previously gold-coated to ascertain electrical conductivity. The micrographs were analyzed through the software Buehler Omnimet. Values, pore size, and porous surface area were obtained, for calculation, a circular-like porous geometry was employed.

3.5 Permeability

The permeation of membrane towards air was measured by Gurley equipment. It is used to measure the air permeation of approximately 6.45 cm^2. A circular area of a membrane using a pressure differential of 1.22 kPa. The recommended range of the liquid column instrument was from 5 to 1800 seconds per 100 mL cylinder displacement.

Gurley permeability values were obtained as followed:

$$Z = \text{time}/(4.1461) \quad \text{Eq 3}$$

$$\text{Gurley permeability, } \mu m \cdot (Pa \cdot s)^{-1} = 135.5/z \quad \text{Eq 4}$$

Where time value is the number of seconds that is needed to permeate an amount of air.

3.6 Mechanical Characterization of precursor films

The annealed polypropylene/calcium carbonate precursors (length: 65 mm; width 60 mm) were prepared, and then tensile measurements along extrusion machine direction were evaluated with a universal testing machine Galdabini Sun 2500. when the conditions were as follows: temperature, 23 °C; and strain rate, 50 mm/min. Three measurements were done for each sample.

4.Results and discussions

4.1 The orientation of precursor films

The structure of the precursor film highly depends on the extrusion condition (temperature, shearing, stretching, and calandering system) and the applied drawing ratio [21, 22]. Also, depends on the chemical nature of the compounds. It is generally agreed that some orientations, either in a plane or out of the plane, will be inducted during the extrusion calandering can be processed through the MEAUS process to produce the flat sheet films.

Several works account for the needing for a highly oriented row lamellar structure in neat polypropylene films, so as membranes could be obtained in the next stages of MEAUS processes; the minimum orientation factor should be above 0.35[20,23]. In the precursor films, the orientation and position of the crystal blocks control the lamellae separation process, which leads to pores formation. The orientation of the crystalline phase of the precursor films has been measured by Fourier-transform infrared spectroscopy.

To determine the optimum annealing conditions that will lead to high orientation and crystallinity, annealing at 140°C was carried out on calcium carbonate compounds. The measured orientation values are written in Table 1. As it can be seen annealing rose the orientation factor of the crystalline phase significantly up. This effect is more marked when 1 wt. % of calcium carbonate was added. Higher amounts of calcium carbonate showed not quite a significant effect on the annealing temperature.

Amorphous phase orientation and average orientation followed the same trend concerning the one showed by the crystalline orientation factor. As annealing is performed, it is suggested that during annealing, the lamellae orient perpendicular to the machine direction. Also, melting of small lamellae and their recrystallization with better orientation can occur. In row nucleated lamellar morphologies, lamellae can be twisted only if both α- and β-axes preferentially orient to the machine direction (MD). Therefore, the observed increase in the F_{am} values and the

consequent increase in the F_c values after annealing demonstrates that annealing can increase the number of twisted lamellae in polypropylene/ calcium carbonate cast film, in other words, the annealing procedure is observed to promote parallel planar lamellae textures.

Orientation factors of our study are showed in Table 2. The addition of talc constrains the orientation of neat polypropylene, being this effect more marked as more amount of talc is added to polypropylene. This observation is different from that observed for injection molding of talc-based composites, in which the concomitance of the orientation of the chains and the talc platelets is a common feature observed in other processes for example injection molding [24,25] tending to align along the flow direction, enhanced by the so-called shear-amplification effect.

Habibi *et al* [26] showed that small shear effects in the MEAUS process rather than in injection molding could explain the reduction in the global orientation of the precursor films when talc is added. Small differences are observed referring to the morphology, particle size, and BET area of talc. Nevertheless, it seems that high aspect ratio talc (more oriented) combined with small particle size and high BET area helps to minimize the descent of orientation factors when higher amounts of talc are added. Probably the increase in talc content leads to some agglomeration of particles, then creates a more spherical-like morphology, that is against a preferential orientation of the polymer when it comes out from the extrusion die.

Holland *et al* [27] showed that at higher (aspect ratio) a platy (upper) boundary is reached and at this boundary, the morphology is essentially a constant and the particle size alone determines the surface area. As talc becomes less platy, the particles form increasingly foliated aggregates. The surface area of talc cannot be directly related to its particle size although the particle size is directly related to the talc morphology and is inversely related to the specific surface area. Hence, talc particles with high aspect ratio filler and also talc particles with micro-lamellar morphology probably are orientated in the PP matrix. Morphological observations by SEM (Figure 1) show that talc samples with higher particle sizes and lower surface areas are constituted by very fine flakes, without arrangement, characteristic of lamellar and micro-lamellar, while talc samples with smaller in particle sizes and higher in surface areas present high aspect ratio and microcrystalline with long, well stacked-up flakes.

The amorphous phase orientation, F_{am}, for annealed precursor film of talc compound showed a very small value compared to the polypropylene and its value considerably decreased. The F_{am} values for the annealed films are also in the same range, and it is seen that annealing treatment has not a major influence on the amorphous phase orientation of talc components. Talc addition might have provoked a constraint of the orientation of the amorphous phase orientation. Therefore, the observed decrease in the F_{am} values and the consequent decrease in the F_c values after annealing demonstrates that annealing can reduce the number of twisted lamellae in polypropylene/ talc compounds.

4.2 Differential scanning calorimetry analysis

Cooling runs carried out on sample pellets displayed that calcium carbonate slightly shifted the crystallization peak temperature to the higher values with respect of neat polypropylene (Table 3), by just adding 1 wt.%. of calcium carbonate; this effect is even more marked as the calcium carbonate content is increased (Figure 3a). Calcium carbonate seems to act as a potential nucleating site that helps to arrange in a more oriented composition along the extrusion direction of the polymer macromolecules.

On the contrary, talc had a large impact on the crystallization behavior for the neat PP (Table 4), which accounts for the high nucleation ability that talc has on the crystallization process of polypropylene. This cooling run displayed that talc rose the crystallinity peak temperature up to 5 ºC concerning the neat polypropylene, by just adding 1 wt.%. of talc (Figure 3b). This effect was even more marked as the talc content was increased (Figure 3c and 3d). Habibi *et al* [26] showed that the size and morphology of the employed talc do not have a significant influence on its nucleation activity. Nevertheless, high contents of the smallest size (E 5936) or more oriented (M HAR) provided the high nucleation efficiency. It is well established in the literature, the nucleation ability that talc has on the crystallization process of polypropylene [17,27].

This nucleation effect is lower than in other works related to this topic; it seems that the high molecular weight polypropylene employed in this work (extrusion grade) restricts the high ability of talc to shift the crystallization onset to higher temperatures. Perego *et al* [28] described that at equal conditions, due to an increase in chain mobility, lower molecular weights have more time to complete crystallization. When talc is present in polypropylene, we suggest that during crystallization only a few polypropylene chains can align themselves on the talc surface, thus causing the apparition of a nucleus site on the mineral surface. The substrate can influence crystallites growth into a particular orientation, which, together with a nuclear density increase, will shorten the duration of the crystallization process.

As indicated in our previous work [26] small differences can be observed, above all at high filler contents, when using talc with small particle size—high BET area, what could be related to the highest available surface area of talc to interact with polypropylene matrix related with the talc nature, talc size, and talc BET area. This could be related to the ability to promote crystalline nuclei. Global crystallization at cooling run conditions showed a reduction in the crystallinity values to neat PP. Being more marked as talc content is increased, as high loads, the filler particles generate a physical barrier to the crystal lamella growth and thus limit the global crystallization efficiency. Even though talc is a good nucleating agent for polypropylene, in this study, we surprisingly can see the reduction in crystallization temperature. The inclusion of talc with small particles into polypropylene might have caused reducing in crystallization temperature and might cause this effect which talc particles may induce heterogeneous nucleation during crystallization and considerably reduced the crystallization of PP/talc as we can see in Table 4 or morphologically, talc might have reduced the spherulite dimension of the PP/talc during crystallization. Although talc particles increased the crystallization temperature compared with that of neat polypropylene.

Figure 3: Nucleating effect of a) calcium carbonate and b, c, d) talc on crystallization peak of polypropylene.

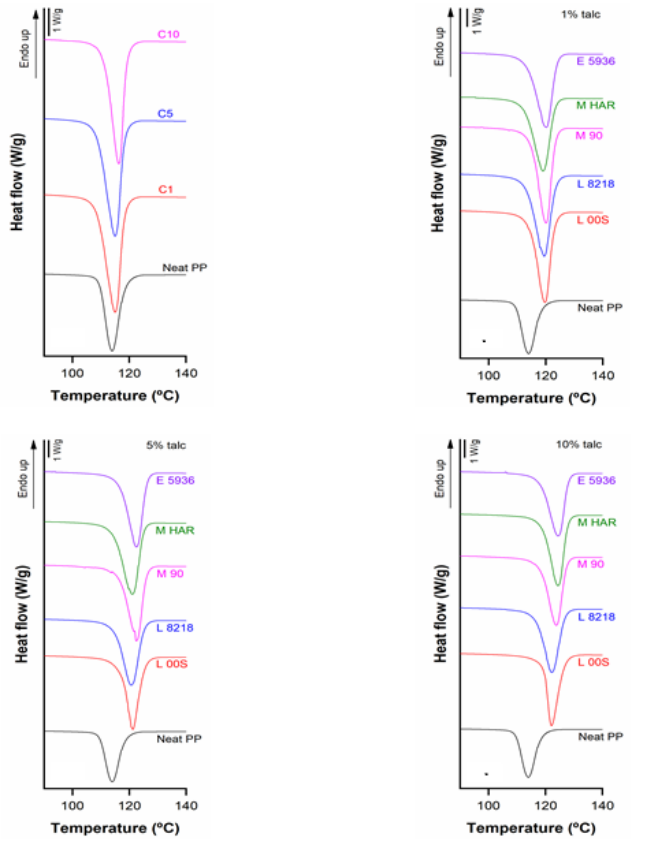

Melting of membranes is analyzed in Figures 4 and 5 as a consequence of the uniaxial strain stage of the MEAUS process, two main effects are observed. Firstly, it can be seen that the secondary shoulder due to annealing has completely disappeared, suggesting that the grown crystals around the initial lamellae during annealing were unstable and could be converted into more stable crystals during stretching [29-31].

Secondly, the melting peak shows a bimodal distribution, with a marked second melting peak (right shoulder) appearing at higher temperatures than the primary melting peak that was observed in non-annealed and annealed precursor films. The main peak belongs to lamellae crystals whereas the right shoulder comes crystals with interconnected bridges between the lamellae [32, 33]. One possible reason could be that some pores are closed due to the break of weak connecting bridges resulting in the appearance of thicker lamellae, and crystals of the interconnected bridges between the lamellae can be leading to the appearance of this shoulder.

This second melting peak appeared in some annealed precursor films, but in a less intense way. The strong bridges under annealing may lead to the appearance of the shoulder, but its content is lower than that of main lamellae crystals, therefore, only a small shoulder can be observed. As will be commented in further morphological section, during the cold and hot stretching step, pores are created and enlarged resulting in the stretching of short and long tie chains. This resulted in a local crystallization, which explains the appearance of interconnected bridges between lamellae, and provokes more intensity in this second melting peak observed in membranes [34, 35].

Figure 4: Melting endotherms for membranes of neat PP and PP/ calcium carbonate.

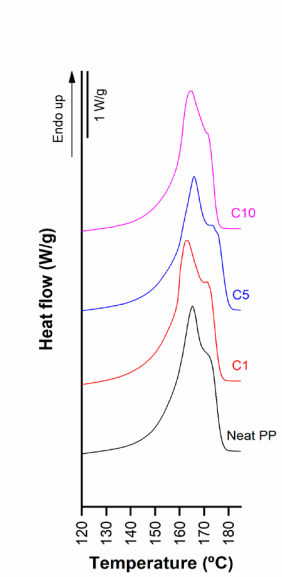

Figure 5: Melting endotherms for membranes of neat PP and PP/talc compounds.

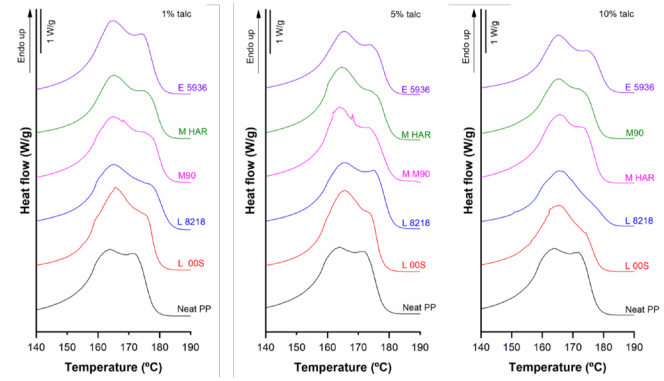

Primary melting peak shifts to a slightly higher temperature in membranes compared to non-annealed and annealed precursor films. When polypropylene is filled, two different behaviors are observed in membranes: whereas calcium carbonate shifts the main melting peak values to lower ones, talc increased the values. As for the calcium carbonate [22], it has explained the shifting of the main melting peak to lower temperatures based on the pulling out of some macromolecules from the initial lamellae. As for the talc effect, this may be due to the melting of very thin lamellae and their recrystallization in the form of thicker ones [22]. No significant changes in this main melting peak have been observed for the amount of filler, nor the talc grade employed.

The secondary melting peak, related to the connecting bridges between lamellae, showed a different behavior depending on the filler employed. Calcium carbonate, showed similar values of neat polypropylene, whereas talc shifted the melting values to higher temperatures. This is related to the strength of these connecting bridges, being stronger

in talc-filled membranes. Non-significant differences were found concerning the amount of filler and the type of talc employed.

The appearance of the secondary melting peak in membranes has as an outcome of increasing the crystallinity values obtained from melting signals when comparing membrane signals to pellet signals Table 3 and 4. The trends of crystallinity values depend on the filler employed. Calcium carbonate leads to higher crystallinity values when compared to non-annealed precursor films, and it is observed that an increase in calcium carbonate content tends to increase crystallinity. On the contrary, an increase in talc content decreases the membrane crystallinity. 1 and 5 wt. % talc membranes showed higher crystallinity values than the annealed precursor films, but 10 wt. % talc membranes inverted this trend.

DSC tests performed on membranes outstands the strong influence of the actual crystallization process that is taking place when producing membrane film precursors through extrusion. Figure 6 a, b displays the different shapes of melting peaks between precursor films. A bimodal distribution is found in membranes. First of all, the interval of temperatures at which melting of membranes takes place is generally broader than the one from precursor films melting. Second, a shoulder attached to the main melting peak appears in membranes. Several works allocate this phenomenon to [23,28] the melting of a secondary crystalline fraction of lesser stability and size, formed during slow isothermal crystallization (annealing stage). This slow crystallization was carried out when annealing the precursor films at 140°C for 15 min previous to the drawing and production of membranes. Surprisingly, the secondary peaks of the talc-based membranes appear at higher temperatures, indicating that talc has promoted more stable and greater crystalline entities during annealing. As we have employed a homopolymer grade of polypropylene the shoulder peak can only be attributed to lamellae distribution (thinner and thicker lamellae). It is assumed that one of these peaks corresponds to crystals of the interconnected bridges between the lamellae and the other reflects the lamellae crystals [36–38].

Figure 6: Precursor films melting endotherms for a) neat PP/$CaCO_3$, b) neat PP/talc compounds.

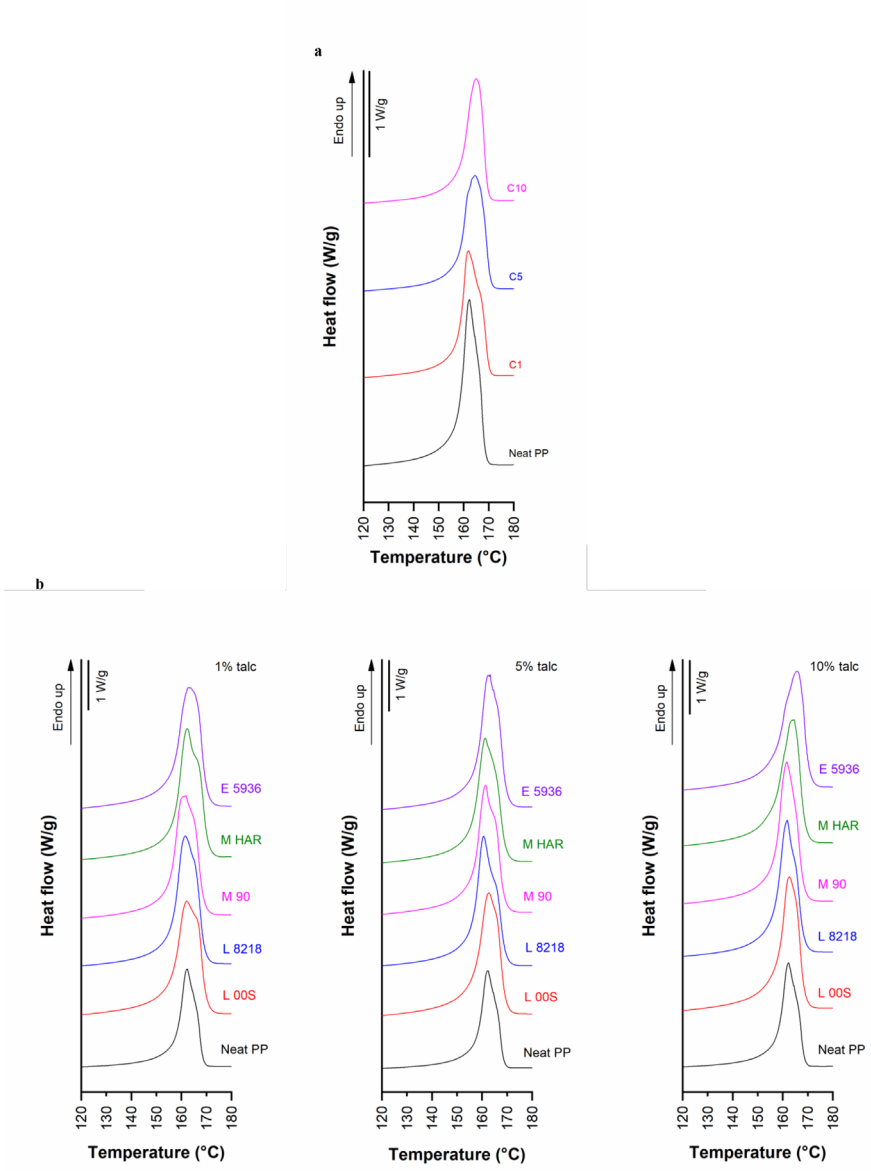

Seguela *et al* [39] reported the transition of the metastable phase to more stable α-PP crystals during the deformation process. They also showed that this endotherm revealed a smectic metastable phase, which was produced when a polypropylene film was extruded and rapidly cooled to room temperature. The smectic phase could transform into monoclinic α-form when annealed at temperatures above 60°C.

Dudic et al [40] illustrated that there was no direct relationship between the endotherm peak and the smectic phase. They attributed the existence to the crystallization of polymer portions which were somewhere between amorphous and smectic phases. Primary melting peak shifts to higher temperatures in membranes concerning precursor films. Talc addition tends to increase this trend. Small differences between the different types of talc are observed, concerning the primary melting peak of membranes, but in the secondary melting peak, there are differences concerning the width of the secondary melting peak, being broader when using microcrystalline talc.

Habibi *et al* [26] described that the appearance of the secondary melting peak has as a consequence an increase in the crystallinity values obtained from melting signals when comparing membrane signals to precursor film signals. Even more interesting is the fact that

in pellets run, talc, hinders crystallization, but in membrane runs, talc enhances crystallization. This is another evidence of the key role of talc during crystallization under strong straining and cooling conditions.

4.3 Morphology of membranes and permeability

A porous morphology was obtained for the different calcium carbonate and talc-based compounds as a consequence of the final MEAUS stage, giving as result porous-based membranes. This final stage consists of a uniaxial stretching divided into two stages: cold strain (room temperature, 50 mm/min and 35 % strain) and hot strain (140ºC, 10 mm/min, 200 % strain). In this stage, it is expected that the lamellae of the row-lamellar structure are forced to get separated, and the length of the connecting bridges between lamellae is increased, leading to an increase of the pore size.

During cold stretching, these chains part convert to initial connecting bridges. Then during hot stretching, some chains are pulled out from the initial lamellae and these stretched chains convert to connecting bridges. This is similar to the melt of crystalline lamellae under tension followed by the re-crystallization into an oriented fibrillar structure [24, 41]. The connecting bridge enlargement process during stretching is proposed by Nilsson et al [42].

It is observed that the addition of 1 wt. % of calcium carbonate resulted in a dramatic increase in the pore-density (Table 4.5). Calcium carbonate could have affected the conversion of stretched chains to connecting bridges during stretching followed by affecting the row-lamellae structure, where the microsecond crystals at the lamellae end could be stronger under a stress field converting to bridges connecting lamellae [43-45]. As a result, the calcium carbonate affected the tensile deformation, which led to having a better chain entanglement and increasing the constraints for tie chains. These connecting bridges result in the better formation of pore structure, and they also contributed to the higher pore density compared to the only polypropylene. The increasing trend within the range 1-10 wt. % calcium carbonate is maintained.

The addition of calcium carbonate caused a gradual increase in pore size, and the porous area might as well show an increase. One of the possible explanations could be because of the presence of calcium carbonate and its debonding with polypropylene, where the lowest amount of pore size belongs to the lowest porous area percentage. Gurley permeability values drastically increased by adding 1 wt. % calcium carbonate, and further filler addition leading to a decrease of Gurley permeability value. One possible effect may be based on the effect of calcium carbonate dispersion, which at higher filler loading, dispersion of the fillers resulting in compacted properties. Also, the presence of calcium carbonate which is intrinsically impermeable occupied the polypropylene networks and reduced the effective spaces for permeation could be another possible explanation.

The synergistic effect of the MEAUS process in filled samples was noticeable due to the combination of the generation of pores, the separation of lamellar blocks, along the debonding mechanisms of calcium carbonate from the polymeric matrix (Figure 7). Both factors led to an increase of permeability for the neat polypropylene, where a maximum of permeability belongs to the membrane with less percentage of calcium carbonate, and as the percentage of calcium carbonate increased the fewer membrane values obtained.

An aspect that has not been possible to be measured is the interconnection state between the pores along the thickness is the important issue, which controls the permeability factor, which interconnected pores determine the membrane performances. This factor may also affect the decrease of permeability at high filler contents, despite the high pore density and high porous area.

The effect of talc on pore morphology and permeability is summarized by all numerical results in Table 4.6, and membrane surface morphology was analyzed in Figures 8 and 9. The pore density of talc-filled samples showed an obvious increase concerning the neat polypropylene as 1 wt.% of talc was added. Further talc content did not yield a significant trend in pore-density. As it is observed, small particle size (range of 1-4 μm) provided high pore-density, whereas bigger particle size notably reduced the pore-density value.

The addition of talc might have affected the conversion of stretched chains to connecting bridges during stretching and affected the row-lamellae structure. As it can be seen an increase in the pore-density compared to the neat polypropylene. Except for the lamellar type talc (L00S), which showed a low value in pore-density, the rest of the talc types showed an increase in pore-density. One possible explanation could be the lamellar talc type might have not affected the tensile deformation to have a better chain entanglement in increasing the constraints for tie-chains. In our previous work [26] we showed that talc might constrain the growth of nucleated pore during the cold strain stage during the drawing of the precursor films, just for the physical barrier of inorganic particles dispersed in a polypropylene matrix. Also,

it can be observed that pore distribution along the membrane surface is much more homogeneous in talc-based membranes rather than in neat polypropylene membranes, in which there are some zones with no pores.

It has been observed that talc addition provoked a remarkable decrease in the crystalline orientation of polypropylene. So, this should affect the creation of pores, due to the lamellae block separation. Nevertheless, in most of the deployed talc types, the pore-density is much higher than the neat polypropylene. The reason that could explain that is the debonding of talc with polypropylene matrix during the stretching stage.

The porous area followed a similar pattern to that of pore-density. In this sense for the studied system, it seems that a particle size range of 3-4 µm provides the best balance of all the studied talc types. The average pore size showed no significant differences.

Pore-density and porous area have a significant effect on permeability. At 1 wt. % talc content, membranes that used talc providing highest values of pore-density and porous area, permeability is the highest. The second factor is talc content. All membranes showed a decreasing trend when talc was high. The reduction of permeability at high talc contents might be related directly to the reduction of permeable area, as these rigid fillers are not permeable to the pass of air.

One of the possible explanations for this reduction in the permeability at high percentages of talc loading could be because talc's particle properties restrict liquid and gas diffusion increasing the diffusion path and impermeability, the highest amount of permeability belongs to the micro-lamellar talc type (M 90) which might be coming from the improvement of stiffness at the lower density when this talc type added to polypropylene. However, the occupation of the polypropylene networks by the presence of talc which might have reduced the effective spaces for permeation could be another possible explanation for the reduction in permeability at the higher talc loadings.

Figure 7: SEM micrographs of neat PP and PP/calcium carbonate membrane, Magnification ×1,000, 10 µm.

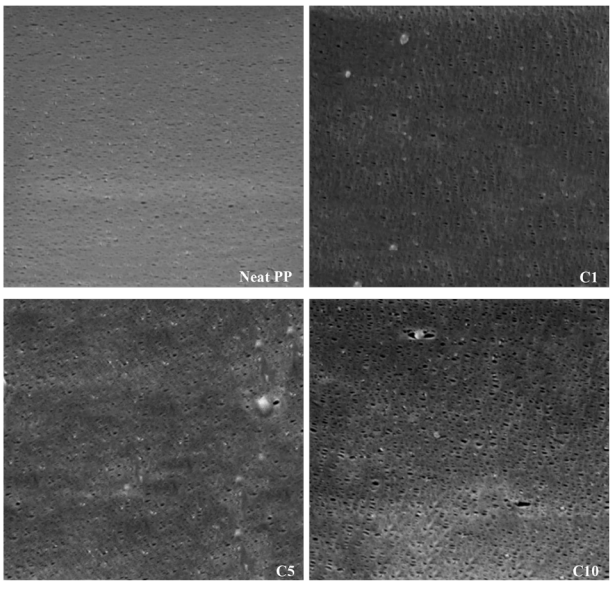

Figure 8: SEM micrographs of neat PP and PP/talc 1 wt.% membranes.

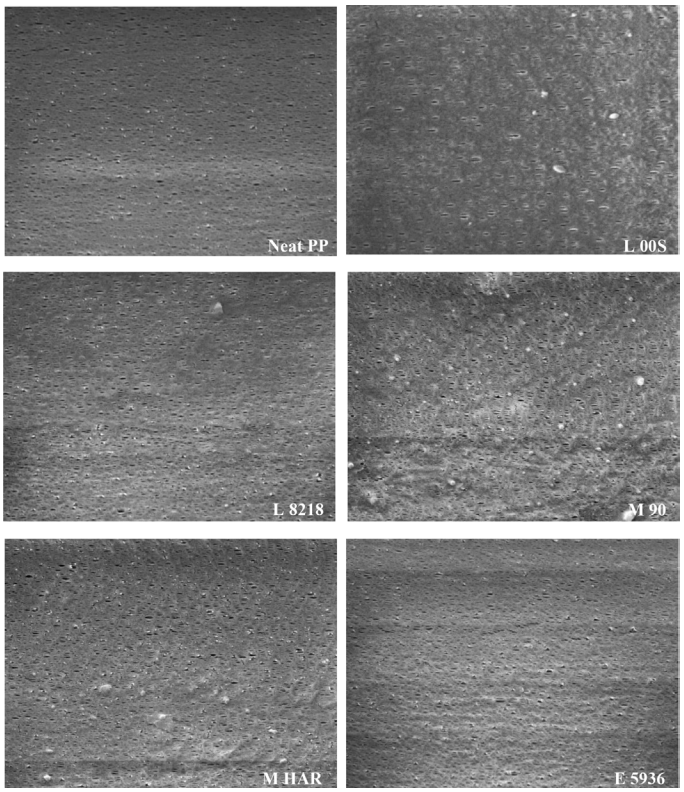

Figure 9: Surface morphologies of M HAR-based membranes with different talc contents.

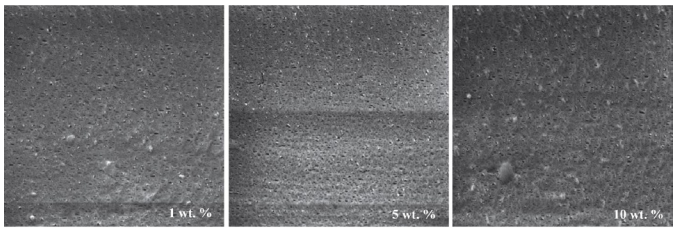

5. Conclusion

For comparison purposes, all the membranes were produced under the same extrusion temperature profile and draw ratio. Differences in orientation, thermal behavior, pore morphology, and permeability are observed with the addition of $CaCO_3$ and talc particles in the polypropylene matrix.

When calcium carbonate increased the crystalline phase orientation, talc grades had a reverse effect. Both trends were even maximized when the filler content was increased. No significant differences in the crystalline orientation factor were observed for the different types of talc employed.

Higher amounts of calcium carbonate showed a not quite significant effect on the annealing temperature. It has been seen that in annealed talc compounds annealing made the orientation factor of the crystalline phase decreased. This decrease is even more noticeable when 1 wt.% of talc was added, referring to the morphology, particle size, and BET

area of talc. High aspect ratio talc (more oriented) combined with small particle size and high BET area helps to minimize the descent of orientation factors when higher amounts of talc are added.

It has been observed that amorphous phase orientation and average orientation in polypropylene/calcium carbonate compounds followed the same trend concerning the one showed by the crystalline orientation factor. The amorphous phase orientation, F_{am}, for annealed precursor film of talc compound showed a very small value compared to the polypropylene and its value considerably decreased. The F_{am} values for the annealed films are also in the same range, and it is seen that annealing treatment has not a major influence on the amorphous phase orientation of talc components. Talc addition might have provoked a constraint of the orientation of the amorphous phase orientation.

The nucleating activity of these fillers was different, talc was the one that showed a higher nucleating ability than calcium carbonate. In the case of talc filler, the size and morphology of the employed talc didn't have a significant influence on its nucleation activity. Nevertheless, high contents of the smallest size (E 5936) or more oriented (M HAR) provided the high nucleation efficiency.

All membranes showed a melting peak from DSC with a bimodal distribution, with the apparition of a right shoulder to the main peak. Calcium carbonate shifted the main melting peak values to lower ones, talc increased the values. Although, small differences between the different types of talc were observed, about the main peak melting temperature of membranes. However, differences were found concerning the width of the shoulder after the main peak melting temperature, being broader when using microcrystalline talc.

The secondary melting peak, related to the connecting bridges between lamellae, showed a different behavior depending on the filler employed. Calcium carbonate, showed similar values of neat polypropylene, whereas talc shifted the melting values to higher temperatures.

During cold stretching, the pores are formed progressively and the initial few pores are from the deterioration crystalline structure, not amorphous regions. Also, for a constant hot stretching level, polypropylene/calcium carbonate compounds showed higher Gurley value and better air permeability than the polypropylene/talc compounds which is related to the constant hot stretching.

The addition of 1 wt. % of calcium carbonate resulted in a dramatic increase in the pore-density. Calcium carbonate also, caused a gradual increase in pore size, and porous area might show an increase in which the lowest amount of pore size belongs to the lowest porous area percentage.

Talc-filled samples showed an increase in the pore density concerning the neat polypropylene as 1 wt.% of talc was added. Further talc content did not yield a significant trend in pore-density. Small particle size (range of 1-4 μm) provided high pore-density, whereas bigger particle size notably reduced the pore-density value. The porous area demonstrated a similar pattern to pore-density. It seems that a particle size range of 3-4 μm provides the best balance of all the studied talc types. Average pore size showed no significant differences in all types of talc.

The highest amount of permeability belongs to the micro-lamellar talc type (M 90) which might be coming from the improvement of stiffness at the lower density when this talc type is added to polypropylene.

ACKNOWLEDGMENTS

The authors would like to acknowledge the Ministerio de Economía, Industria y Competitividad (Government of Spain) for the financial support of project MAT2017-89787-P.

References

1. R. W. Baker, Membrane Technology and Applications, Wiley, Chichester, UK 2004.
2. F. Sadeghi, A Ajji, P J Carreau, J Membr Sci. 2007; 292: 62.
3. F. Sadeghi, A. Ajji, P. J. Carreau, J. Polym. Sci. B Polym. Phys. 2008, 46, 148.
4. S H Tabatabaei, Development of microporous membranes from PP/HDPE films through cast extrusion and stretching. 2009; 345:148-159.
5. S H Tabatabaei, P J Carreau, A Ajji J. Membr. Sci. 2008; 325: 772.
6. F Sadeghi, A Ajji, P J Carreau. Analysis of row nucleated lamellar morphology of polypropylene obtained from the cast film process: Effect of melt rheology and process conditionsPolym. Eng. Sci. 2007; 47(7): 1170-1178.
7. L Caihong, H Weiliang, X Ruijie, X Yunqi, J Plast Film Sheet. 2012; 28: 151.
8. S Nakamura, S Kaneko, Y Mizutani, J. Appl Polym. Sci. 1993; 49: 143.
9. S. Nagō, Y. Mizutani. Microporous polypropylene sheets containing CaCO3 filler: Effects of stretching ratio and removing CaCO3 filler. J Appl Polym. Sci. 1998; 68(10): 1543-1553.
10. A Saffar, P J Carreau, A Ajji, M R Kamal, J. Membr. Sci. 2014; 462: 50.
11. A Qaiss, H Saidi, O Fassi-Fehri, M Bousmina. Cellular polypropylene-based piezoelectric films. J Appl Polym Sci. 2012; 52(12): 3425.
12. J. Zhang, J. Fang, J. L. Wu, J. Wu, H. Mo, Z. M. Ma, N. L. Zhou, J. Shen, Polym. Compos. 2011, 32: 2637-2644.
13. L Caihong, Q Cai, R Xu, X Chen, J Xie. Influence of magnesium sulfate whiskers on the structure and properties of melt-stretching polypropylene microporous membranes. J Appl. Polym Sci. 2016; 133(35): 43884.
14. Q Cai, R Xu, X Chen, C Chen, H Mo, C Lei. Polym. Compos. 2016; 37, 2684.
15. J Velasco, J De Saja, A Martinez, J. Crystallization behavior of polypropylene filled with surface-modified talcAppl. Polym. Sci. 1996; 61(1): 125-132.
16. M Xanthos, C Chandavasu, K Sirkar, C Gogos, Melt processed microporous films from compatibilized immiscible blends with

potential as membranes. Polym Eng Sci. 2002; 42(4): 810-825.

17. L J Michot, F Villieras, M Francois, J Yvon, R Le Dred, J M Cases. The Structural Microscopic Hydrophilicity of Talc. Langmuir. 1994; 10(10): 3765-3773.
18. B Rotenberg, A J Patel, D Chandler. Molecular explanation for why talc surfaces can be both hydrophilic and hydrophobic. J Am Chem Soc. 2011; 133(50): 20521-20527.
19. I M Ward, P D Coates, M M Dumoulin, Solid Phase Processing of Polymers, Hanser, 2000;
20. S H Tabatabaei, P J Carreau, A Ajji. Polymer. 2009; 50: 4228.
21. K Ishikiriyama, B Wunderlich, Crystallization and melting of poly(oxyethylene) analyzed by temperature-modulated calorimetry. J Polym Sci. B Polym. Phys. 1997; 35(12): 1877-1886.
22. M Kamal, C S Sharma, P Upadhyaya, V Verma, K N Pandey, V Kumar, et al. Calcium carbonate (CaCO3) nanoparticle filled polypropylene: Effect of particle Surface treatment on mechanical, thermal, and morphological performance of composites. J Appl Polym Sci. 2012; 124(4): 2649-2656.
23. E Ferrage, F Martin, S Petit, S Pejo-Soucaille, P Micoud, G Fourty, J Fortune, et al. Evaluation of talc morphology using FTIR and H/D, Clay Minerals. 2003; 38(2): 141-150, (2003).
24. M Alonso, J Velasco, Constrained crystallization and activity of filler in surface modified talc polypropylene composites. European Polymer Journal.1997; 33(3): 255-262,
25. S Guo, Chinese J Polym Sci. 2015; 33: 1028.
26. K Habibi, P Castejón, A B Martínez, D Arencón. Adv Polym Technol, 2018; 37: 3315.
27. H Holland, M Murtagh, Adv. X-ray Anal. 2000; 42, 421.
28. G Perego, G D Cella, C Bastioli, Effect of molecular weight and crystallinity on poly (lactic acid) mechanical properties. J Appl Polym Sci. 1996; 59(1): 37-43.
29. S Lee, S Park, H Song. Lamellar crystalline structure of hard elastic HDPE films and its influence on microporous membrane formation. Polymer. 2006; 47(10): 3540-3547.
30. C Xiande, X Ruijie, X Jiayi, L Yuanfei, L. Caihong, L. Liangbin et al. the study of room-temperature stretching of annealed polypropylene cast film with row-nucleated crystalline structure. Polymer. 2016; 94(566): 31-42.
31. Guo Shaoyun. Fabrication of microporous membranes from melt extruded polypropylene precursor films via stretching: Effect of annealing, Polymer Science: English version. 2015; 33: 1028-1037.
32. CH Lei, SQ Wu, RJ Xu, Q Cai, B Hu, XL Peng, WQ Shi. Formation of stable crystalline connecting bridges during hot stretching of polypropylene hard elastomer film, Polym Bull. 2013; 70(4):1353-1366.
33. C Qi, X Ruijie, W Shuqiu, Ch Changbin, M Haibin, L Caihong, Influence of annealing temperature on the lamellae and connecting bridge structure of stretched polypropylene microporous membrane, Polym Int. 2015; 64 (3): 446-452.
34. XD Chen, RJ Xu, JY Xie, CH Lei, The study of room-temperature stretching of annealed polypropylene cast film with row-nucleated crystalline structure, Polymer. 2016; 94:31-42.
35. SQ Wu, CH Lei, Q Cai, RJ Xu, B Hu, WQ Shi, XL Peng, et al. Study of structure and properties of polypropylene microporous membrane only by hot stretching, Polym Bull. 2014; 71(9): 2205-2217.
36. R H Rane, K Jayaraman, K L Nichols, T R Bieler, M H Mazor. Evolution of Crystalline Orientation and Texture during Solid Phase Die-Drawing of PP-Talc Composites, J Polym. Sci B Polym Phys. 2014; 52(23): 1528-1538.
37. F Qiu, M Wang, Y Hao, S Guo. The effect of talc orientation and transcrystallization on mechanical properties and thermal stability of the polypropylene/talc composites, Compos. Part A Appl Sci Manuf. 2014; 58, 7-15.
38. A Makhlouf, H Satha, D Frihi, S Gherib, R Seguela. Optimization of the crystallinity of polypropylene/submicronic-talc composites: The role of filler ratio and cooling rate, Express Polym. Lett. 2016; 10(3): 237-242.
39. R Seguela, E Staniek, B Escaig. Plastic deformation of polypropylene in relation to crystalline structure. J Appl Polym Sci.1999; 71(11): 1873-1885.
40. D Dudic, D Kostoski, V Djokovic. Formation and behavior of low-temperature melting peak of quenched and annealed isotactic polypropylene, Polym. Int. 2002; 51:111-116.
41. M Xanthos, C Chandavasu, K Sirkar, C Gogos. Melt processed microporous films from compatibilized immiscible blends with potential as membranes. Polymer Engineering & Science. 2002; 42(4): 810-825.
42. F Nilsson, X Lan, T Gkourmpis, M S Hedenqvist, U W Gedde. Modelling tie chains and trapped entanglements in polyethylene. Polymer. 2012; 53(16): 3594-3601.
43. JA Degroot, AT Doughty, KB Stewart. Effects of cast film fabrication variables on structure development and key stretch film properties. J Appl Polym Sci.1994; 52(3): 365-376.
44. RJ Xu, XD Chen, JY Xie, Q Cai, CH Lei. Influence of melt-draw ratio on the crystalline structure and properties of polypropylene cast film and stretched microporous membrane. Ind Eng Chem Res. 2015; 54(11): 2991-2999.
45. A Saffar, PJ Carreau, MR Kamal, A Ajji. Hydrophilic modification of polypropylene microporous membranes by grafting TiO2 nanoparticles with acrylic acid groups on the surface. Polymer. 2014; 55(23): 6069-6075.